

VELOCITY/MIXTURE FRACTION STATISTICS OF ROUND, SELF-PRESERVING, BUOYANT TURBULENT PLUMES

by

Z. Dai,¹ L.-K. Tseng² and G.M. Faeth³
 Department of Aerospace Engineering
 The University of Michigan
 Ann Arbor, Michigan 48109-2118, U.S.A.

ABSTRACT

An experimental study of the structure of round buoyant turbulent plumes was carried out, limited to conditions in the self-preserving portion of the flow. Plume conditions were simulated using dense gas sources (carbon dioxide and sulfur hexafluoride) in a still and unstratified air environment. Velocity/mixture-fraction statistics, and other higher-order turbulence quantities, were measured using laser velocimetry and laser-induced fluorescence. Similar to earlier observations of these plumes, self-preserving behavior of all properties was observed for the present test range, which involved streamwise distances of 87-151 source diameters and 12-43 Morton length scales from the source. Streamwise turbulent fluxes of mass and momentum exhibited countergradient diffusion near the edge of the flow, although the much more significant radial fluxes of these properties satisfied gradient diffusion in the normal manner. The turbulent Prandtl/Schmidt number, the ratio of time scales characterizing velocity and mixture fraction fluctuations and the coefficient of the radial gradient diffusion approximation for Reynolds stress, all exhibited significant variations across the flow rather than remaining constant as prescribed by simple turbulence models. Fourth moments of velocity and velocity/mixture fraction fluctuations generally satisfied the quasi-Gaussian approximation. Consideration of budgets of turbulence quantities provided information about kinetic energy and scalar variance dissipation rates, and also indicated that the source of large mixture fraction fluctuations near the axis of

these flows involves interactions between large streamwise turbulent mass fluxes and the rapid decay of mean mixture fractions in the streamwise direction.

NOMENCLATURE

a	=	acceleration of gravity
B_0	=	source buoyancy flux
C_{g2}	=	turbulence modeling constant, Eq. (20)
C_μ	=	turbulence modeling constant, Eq. (21)
d	=	source diameter
D, D_g	=	turbulent diffusion of k and g , Eqs. (13) and (18)
f	=	mixture fraction
$F(\eta)$	=	scaled radial distribution of \bar{f} , Eqs. (3) and (5)
Fr_0	=	source Froude number = $(4/\pi)^{1/4} \rho_M/d$
g	=	variance of mixture fraction fluctuations = \bar{f}'^2
G	=	buoyant production of k , Eq. (16)
k	=	turbulence kinetic energy
k_f, k_u	=	plume width coefficients based on \bar{f} and \bar{u} , Eq. (6)
ρ_f, ρ_u	=	characteristic plume radii based on \bar{f} and \bar{u} , Eq. (6)
ρ_M	=	Morton length scale, $M_0^{3/4} / B_0^{1/2}$
M_0	=	source specific momentum flux
P, P_g	=	mechanical production of k and g , Eqs. (15) and (19)
r	=	radial distance
Re_0	=	source Reynolds number = $u_0 d / \nu_0$
T	=	pressure diffusion of k , Eq. (14)
u	=	streamwise velocity

¹Graduate Student Research Assistant.

²Research Fellow, currently with School of Mechanical Engineering, Purdue University, West Lafayette, Indiana.

³Professor, Fellow ASME.

- $U(\eta)$ = scaled radial distribution of \bar{u} , Eqs. (2) and (5)
 v = radial velocity
 w = tangential velocity
 x = streamwise distance
 ϵ, ϵ_g = rate of dissipation of k and g
 η = dimensionless radial distance, $r/(x-x_0)$
 ν = molecular kinematic viscosity
 ν_t = effective turbulence kinematic viscosity
 ρ = density
 σ_T = effective turbulence Prandtl/Schmidt number
 ϕ_i = generic variable
Subscripts
 c = centerline value
 o = initial value or virtual origin location
 ∞ = ambient value
Superscripts
 $(\bar{\quad})$ = time-averaged mean value
 $(\bar{\quad})'$ = root mean-squared fluctuating value

INTRODUCTION

The structure of round buoyant turbulent plumes in still and unstratified environments is a classical problem that has attracted significant attention in order to gain a better understanding of buoyancy/turbulence interactions, see Chen and Rodi (1980), Kotsovinos (1985), List (1982), Papanicolaou and List (1987, 1988) and references cited therein for summaries of past turbulent plume studies. In general, most investigations of this flow have emphasized the fully-developed region where effects of the source have been lost and flow properties become self-preserving, in order to simplify both theoretical considerations and the interpretation of measurements (Morton, 1959; Morton et al., 1956; Rouse et al., 1952; Tennekes and Lumley, 1972). Motivated by these observations, measurements of mean and fluctuating velocities and scalar properties in self-preserving round buoyant turbulent plumes were recently completed in this laboratory (Dai et al., 1994, 1995). The objectives of the present investigation were to extend these measurements to consider additional turbulence properties needed to develop both improved theoretical

understanding and modeling capabilities for buoyant turbulent flows.

Buoyant jets were used as the source of the present round buoyant turbulent plumes, similar to most past studies of this flow. Then, all scalar properties are conveniently represented as functions of the mixture fraction (which corresponds to the mass fraction of source material in a sample) called state relationships (Dai et al., 1994, 1995). Additionally, reaching self-preserving conditions for buoyant jet sources requires streamwise distances that are large in comparison to both the source diameter, d , as a measure of conditions where source disturbances have been lost, and the Morton length scale, l_M , as a measure of conditions where the buoyant features of the flow are dominant (Morton, 1959; List, 1982; Papanicolaou and List, 1988). When these requirements are satisfied, $f \ll 1$ so that the state relationship giving the density as a function of mixture fraction can be linearized as follows (Dai et al., 1994, 1995):

$$\rho = \rho_\infty + f\rho_o(1-\rho_\infty/\rho_o), \quad f \ll 1 \quad (1)$$

Noting that the buoyancy flux of the plume, B_o , is conserved, mean streamwise velocities and mixture fractions can be scaled as follows for self-preserving conditions (Dai et al., 1995; List, 1982):

$$\bar{u}((x-x_o)/B_o)^{1/3} = U(\eta) \quad (2)$$

$$\bar{f} a B_o^{-2/3} (x-x_o)^{5/3} |d(\ln \rho)/df|_{f \rightarrow 0} = F(\eta) \quad (3)$$

where from Eq. (1)

$$|d(\ln \rho)/df|_{f \rightarrow 0} = |\rho_o - \rho_\infty|/\rho_o \quad (4)$$

The functions $U(\eta)$ and $F(\eta)$ generally are approximated by Gaussian fits, as follows (Rouse et al., 1952; Papanicolaou and List, 1988; Mizushima et al., 1979; Ogino et al., 1980; Shabbir and George, 1992; George et al., 1977):

$$\begin{aligned} U(\eta) &= U(0)\exp(-(k_u\eta)^2), \\ F(\eta) &= F(0)\exp(-(k_f\eta)^2) \end{aligned} \quad (5)$$

where

$$k_u = (x-x_0)/\ell_u, \quad k_f = (x-x_0)/\ell_f \quad (6)$$

and ℓ_u and ℓ_f are characteristic plume radii where $\bar{u}/\bar{u}_c = \bar{f}/\bar{f}_c = \exp(-1)$, respectively.

Following the classical experimental study of round buoyant turbulent plumes of Rouse et al. (1952), where source properties and thus estimates of $(x-x_0)/d$ and $(x-x_0)/\ell_M$ are difficult to define, attempts generally have been made to carry out measurements at increasing distances from the source in order to more closely approach self-preserving conditions, see Abraham (1960), Seban and Behnia (1976), Nagagome and Hirata (1977), Zimin and Frik (1979), Mizushima et al. (1979), Ogino et al. (1980), Shabbir and George (1992), Peterson and Bayazitoglu (1992), Papanicolaou and List (1987, 1988), Papantoniou and List (1989) and Dai et al. (1994, 1995). Except for the measurements of Papantoniou and List (1989) and Dai et al. (1994, 1995), to be discussed subsequently, however, these measurements were limited to $(x-x_0)/d \leq 62$, which seems rather small to achieve self-preserving behavior compared to nonbuoyant jets where $(x-x_0)/d \geq 60$ generally is required to reach self-preserving behavior for both mean and fluctuating properties, see Hinze (1975), Panchapakesan and Lumley (1993a,b), Tennekes and Lumley (1972) and references cited therein. Thus, not surprisingly, recent measurements of Papantoniou and List (1989) and Dai et al. (1994, 1995) found that self-preserving behavior of mean and fluctuating velocities and mixture fractions only was achieved when $(x-x_0)/d$ and $(x-x_0)/\ell_M$ were greater than roughly 90 and 12, respectively. These results also showed that self-preserving round buoyant turbulent plumes were narrower, with larger values of mean velocities and both mean and fluctuating mixture fractions near the axis (when appropriately scaled), than earlier reported measurements of self-preserving properties made closer to the source. For example, values of characteristic plume radii were reduced up to 40%, and corresponding values of $U(0)$ and $F(0)$ were increased up to 40%, over the range of the experiments mentioned earlier (Dai et al., 1994, 1995). It seems likely that self-preserving behavior for

other properties only is achieved at comparable conditions.

In view of the previous discussion, additional measurements within the self-preserving region of round buoyant turbulent plumes clearly are needed in order to supplement the results available from Papantoniou and List (1989) and Dai et al. (1994, 1995). Thus, the present objectives were to carry out a study along these lines, involving new measurements of velocity/mixture function statistics and other higher-order turbulence quantities, using the experimental conditions of Dai et al. (1994, 1995). These results were also exploited to complete conservation checks of the experiments of Dai et al. (1994, 1995), to compute budgets of turbulence quantities, and to begin assessment of contemporary models of buoyant turbulent flows. The test conditions of Dai et al. (1994, 1995) were considered, which involved round source flows of carbon dioxide and sulfur hexafluoride in still air at room temperature and atmospheric pressure. Thus, these conditions yield downward-flowing round buoyant turbulent plumes in still and unstratified environments, while providing a straightforward specification of plume buoyancy fluxes. Instrumentation also followed Dai et al. (1994, 1995) with laser velocimetry (LV) used to measure velocities and laser-induced iodine fluorescence (LIF) used to measure mixture fractions.

EXPERIMENTAL METHODS

Test Apparatus. Descriptions of the experimental apparatus, instrumentation and test conditions will be brief, see Dai et al. (1994, 1995) for more details. The test plumes were observed in a screened enclosure, that could be traversed to accommodate rigidly-mounted instrumentation, which was mounted within an outer enclosure. The outer enclosure had plastic side walls with a screen across the top for air inflow in order to compensate for the removal of air entrained by the plume. The plume flow was removed through ducts located at the lower corners of the outer enclosure using a bypass/damper system to match plume entrainment rates. Effects of coflow and confinement on flow properties were evaluated and found to be negligible. All components that might contact iodine vapor were plastic, painted

or sealed in plastic wrap, in order to prevent corrosion.

The plume sources consisted of long rigid round plastic tubes that could be traversed in the vertical direction to accommodate measurements at various streamwise distances from the source. Gas flows to the sources were controlled and measured using pressure regulators in conjunction with critical flow orifices. The source flows were seeded with iodine vapor for LIF measurements. The ambient air was seeded with oil drops (roughly 1 μm nominal diameter) for LV measurements using several multiple jet seeders that discharged above the screened top of the outer enclosure. Maximum mixture fractions in the self-preserving region were less than 6%; therefore, effects of concentration bias, because only the ambient air was seeded, were negligible.

Instrumentation. The combined LV/LIF measuring system was similar to the arrangement described by Lai and Faeth (1987). A dual-beam, frequency-shifted LV was used for velocity measurements. The arrangement was based on the 514.5 nm line of an argon-ion laser, and had a horizontal optical axis and a measuring volume diameter and length of 400 and 260 μm , respectively. Various orientations of the plane of the laser beams, the direction of the optical axis and the direction of horizontal traverse of the plumes, were used to resolve various correlations of velocity and mixture fraction fluctuations, as described by Lai and Faeth (1987). The detector output was processed using a burst-counter signal processor. The low-pass-filtered analog output of the signal processor was sampled at equal time intervals in order to avoid problems of velocity bias, while directional bias and ambiguity were controlled by frequency-shifting. The processor output was sampled at rates more than twice the break frequency of the low-pass-filter in order to control alias signals. Seeding levels were controlled so that effects of step noise contributed less than 3% to determinations of velocity fluctuations (Dai et al., 1995). Experimental uncertainties (95% confidence) are estimated to be less than 5, 10, 15 and 20%, for first-, second-, third- and fourth-order moments of particular components of velocity fluctuations, respectively; uncertainties of corresponding moments involving several components of velocity fluctuations are generally larger, up to

twice as large. These uncertainties were maintained up to $r/(x-x_0) = 0.15$ but increased at larger radial distances, roughly inversely proportional to \bar{u} .

The LIF signal was produced by the fluorescence of iodine in the 514.5 nm laser beams used for LV. The detector was positioned at right angles to the optical axis to yield a measuring volume diameter and length of 260 and 1000 μm , respectively. The LIF signal was separated from the light scattered at the laser line using a long-pass optical filter with a cut-off wavelength of 530 nm. The detector output was amplified and low-pass filtered to control alias signals using a sixth-order Chebychev filter having a break frequency of 500 Hz. The absorption and LIF signals were calibrated based on measurements across the source exit by mixing the source flow with air to simulate various mixture fractions. These calibrations showed that iodine seeding level fluctuations were less than 1%, that the LIF signal varied linearly with laser power and iodine concentration, and that reabsorption of scattered light was negligible. Differential diffusion effects between the source gas (carbon dioxide or sulfur hexafluoride) and iodine also are negligible, as discussed by Dai et al. (1994). Analysis of experimental uncertainties indicated values less than 5, 10, 15 and 20% for first-, second-, third- and fourth-order moments of mixture-fraction fluctuations, respectively. These uncertainties were maintained up to $r/(x-x_0) = 0.15$ but increased at larger radial distances, roughly inversely proportional to \bar{f} . As before, uncertainties of moments involving several components of velocity and mixture-fraction fluctuations are larger, up to 50% larger.

Test Conditions. The test conditions for the carbon dioxide and sulfur hexafluoride plumes are summarized in detail by Dai et al. (1994, 1995). Major parameters for the carbon dioxide and sulfur hexafluoride sources, respectively, are as follows: $d = 9.7$ and 6.4 mm, $\rho_0/\rho_\infty = 1.51$ and 5.06, $Re_0 = 2000$ and 4600, $Fr_0 = 7.80$ and 3.75 and $\rho_M/d = 7.34$ and 3.53. The virtual origins of the two flows were relatively small, i.e., $x_0/d < 12.7$.

Present measurements and those of Dai et al. (1994, 1995) were used to complete conservation checks along the lines of Shabbir and Taulbee (1990). The results showed that these measurements satisfied the governing equations within experimental uncertainties. In addition, buoyancy fluxes were conserved within 5% and the balance between the plume momentum and buoyancy terms in the integrated form of the governing equation for conservation of momentum was satisfied within an average of 18%, which is acceptable in view of the experimental uncertainties (particularly near the edge of the flow).

RESULTS AND DISCUSSION

Results will be presented by considering second-, third- and fourth-moments of fluctuating quantities, in turn, before concluding with a discussion of budgets of turbulence quantities. It should be noted at the outset that all properties measured during the present investigation exhibited self-preserving behavior over the test range, e.g., $87 \leq (x-x_0)/d \leq 151$ and $12 \leq (x-x_0)/\ell_M \leq 43$, which agrees with the earlier observations of other mean and turbulent quantities of Dai et al. (1994, 1995).

Second Moments. Mean quantities (e.g., \bar{f} , \bar{u} and \bar{v}), some second moments of fluctuating quantities (e.g., \bar{f}'^2 , \bar{u}'^2 , \bar{v}'^2 , \bar{w}'^2 and $\overline{u'v'}$) and associated quantities (e.g., probability density functions, spatial correlations, temporal power spectra and temporal and spatial integration scales) can be found in Dai et al. (1994, 1995). Other similar parameters at this level (e.g., \bar{w} , $\overline{w'v'}$ and $\overline{w'u'}$) are formally zero. Thus, present measurements of second moments concentrated on combined mixture fraction/velocity correlations (e.g., the turbulent mass fluxes, $\overline{f'u'}$, $\overline{f'v'}$ and $\overline{f'w'}$, and the turbulent Prandtl/Schmidt number).

Present measurements of the turbulent mass fluxes, $\overline{f'u'}$, $\overline{f'v'}$ and $\overline{f'w'}$, are illustrated in Fig. 1. The tangential turbulent mass flux, $\overline{f'w'} = 0$, for an axisymmetric flow which was adequately represented by present measurements. The radial turbulent mass flux, $\overline{f'v'}$, is the most

important turbulent mass diffusion parameter in the present boundary-layer-like flow. Similar to $\overline{u'v'}$ discussed by Dai et al. (1995), $\overline{f'v'} = 0$ at $r=0$ due to symmetry, and then increases to a maximum near $r/(x-x_0) = 0.06$ (in the absolute sense) before decreasing to zero once again at large r . Finally, $\overline{f'u'}$ exhibits rather large values in the present flows, somewhat analogous to \bar{u}'^2 and \bar{f}'^2 discussed by Dai et al. (1994, 1995). In fact, the correlation coefficient $(\overline{f'u'}/(\bar{f}'\bar{u}'))_c \approx 0.7$, which is unusually large. This behavior is caused by the intrinsic instability of plumes, where large values of f provide a corresponding potential to generate large values of u through effects of buoyancy (George et al., 1977).

Another aspect of the large values of $\overline{f'u'}$ is that the turbulent mass flux contribution to the total buoyancy flux of the plume is appreciable (roughly 15%) and must be considered in conservation checks.

The consistency of present measured values of $\overline{f'v'}$ was evaluated similar to earlier considerations of \bar{v} and $\overline{u'v'}$ by Dai et al. (1995). Imposing the approximations of a boundary-layer-like flow, self-preserving conditions so that density variations are small, and neglecting molecular mass diffusion in comparison to turbulent mass diffusion, the governing equation for mean mixture fraction becomes:

$$\begin{aligned} \bar{u} \partial \bar{f} / \partial x + \bar{v} \partial \bar{f} / \partial r &= - \partial / \partial x (\overline{f'u'}) \\ &= - \partial / \partial r (r \overline{f'v'}) / r \end{aligned} \quad (7)$$

Then, integrating Eq. (7), both ignoring and considering the streamwise turbulent mass flux, $\overline{f'u'}$, and using correlations of \bar{u} , \bar{v} and \bar{f} in the self-preserving portion of the flow from Dai et al. (1994, 1995), yields the two predictions of $\overline{f'v'}$ illustrated in Fig. 1. Including $\overline{f'u'}$ in the integration does not have a large effect on predictions of $\overline{f'v'}$ because even though $\overline{f'u'}$ is large near the axis, $\overline{f'v'}$ is small in this region due to the requirements of symmetry. Thus, both predictions are in good agreement with present measurements of $\overline{f'v'}$ which helps to

confirm the internal consistency of the measurements.

The gradient diffusion approximation is commonly made for simplified models of turbulent mixing, which implies the following relationships for the radial and streamwise turbulent mass fluxes:

$$\overline{f'v'} = - (v_T/\sigma_T) \partial \bar{f}/\partial r, \quad \overline{f'u'} = - (v_T/\sigma_T) \partial \bar{f}/\partial x \quad (8)$$

This approach is generally acceptable for the radial direction, based on present measurements of $\overline{f'v'}$ illustrated in Fig. 1 and the correlation for \bar{f} given by Eqs. (3) and (5). Unfortunately, the approach yields estimates of countergradient diffusion in the streamwise direction, e.g., $\overline{f'u'} > 0$ from Fig. 1 but $\partial \bar{f}/\partial x \geq 0$ when $r/(x-x_0) \geq (5/6)^{1/2}/k_f = 0.082$ which implies an unphysical negative value of v_T near the edge of the flow as well as a clear absence of the isotropy of v_T implied by Eq. (8). Analogous considerations for turbulent stresses, based on the measurements of Dai et al. (1995), again yield acceptable behavior for the radial direction; however, countergradient diffusion is encountered for the streamwise direction when $r/(x-x_0) \geq (1/6)^{1/2}/k_u = 0.042$. Naturally, these countergradient diffusion effects in the streamwise direction are not very important for boundary layer flows like the present plumes, where streamwise turbulent transport is ignored in any event; nevertheless, this deficiency raises concerns about the use of simple gradient diffusion hypotheses for more complex buoyant turbulent flows of interest in practice.

Simple gradient diffusion hypotheses, with constant turbulent Prandtl/Schmidt numbers, are even problematical for transport in the radial direction within self-preserving buoyant turbulent plumes. For example, introducing the gradient diffusion hypotheses for the Reynolds stress, as follows:

$$\overline{u'v'} = - v_T \partial \bar{u}/\partial r \quad (9)$$

and eliminating v_T between Eq. (9) and the expression for $\overline{f'v'}$ in Eq. (8), yields the following expression for the turbulent Prandtl/Schmidt number:

$$\sigma_T = (\overline{u'v'}/\overline{f'v'}) (\partial \bar{f}/\partial r) / (\partial \bar{u}/\partial r) \quad (10)$$

The available measurements of $\overline{u'v'}$, $\overline{f'v'}$, \bar{f} and \bar{u} from Dai et al. (1994, 1995) and the present study were used to find σ_T as a function of radial position in the self-preserving region of the flow as illustrated in Fig. 2. The measurements exhibit significant scatter, which is unavoidable because finding σ_T involves four measurements including two determinations of gradients. Keeping this limitation in mind, the results indicate crude self-preserving behavior for σ_T , with σ_T near 0.8 at $r=0$ decreasing progressively with increasing radial distance toward $\sigma_T \approx 0.1$ near the edge of the flow (except for a few outlying points at the flow edge where present experimental uncertainties are large). Clearly, this behavior departs significantly from assumptions of $\sigma_T = 0.7$ or 0.9 across the width of the flow made in simple turbulence models, see Lockwood and Naguib (1975), Lumley (1978), Shabbir and Taulbee (1990), Taulbee (1992) and references cited therein. Thus, the difficulty with σ_T also suggests that higher-order turbulent closures are needed to reliably treat flow development effects in buoyant turbulent flows.

Third Moments. Gradients of third moments of velocity fluctuations determine the turbulent diffusion of turbulence kinetic energy and turbulent stresses, and are important for estimating the turbulence kinetic energy budget and developing higher-order models of turbulence (Malin and Younis, 1990; Panchapakesan and Lumley, 1993a,b; Shih et al., 1987). For the present flows, several of these correlations are zero due to axial symmetry, e.g., $\overline{w'u'^2} = \overline{w'v'^2} = \overline{w'^3} = 0$; of these, the last was observed and was found to be properly equal to zero as a check of the measurements.

Measurements of all other third moments of velocity fluctuations — $\overline{u^3}$, $\overline{v^3}$, $\overline{u^2v}$, $\overline{u'v'^2}$, $\overline{v'w'^2}$ and $\overline{u'w'^2}$ — were completed and are illustrated in Fig. 3, after normalizing in a manner appropriate for round self-preserving buoyant turbulent plumes. As noted earlier, these results exhibit self-preserving behavior within experimental uncertainties. The various correlations also have been approximated by local least squares fits in preparation for the calculation of budgets to be discussed later. Panchapakesan and Lumley (1993a) report recent measurements of these moments, and discuss earlier measurements as well, for round nonbuoyant turbulent jets; they find maximum values of $\overline{u^3}$ and $\overline{v^3}$ at $\sim r/(x-x_0) \approx 0.1$ with a maximum value of $\overline{v^3}/\overline{u^3}$ of 0.002, similar to the present measurements. Nevertheless, maximum values of $\overline{u^3}/\overline{u_c^3}$ are somewhat larger for nonbuoyant than buoyant turbulent flows, 0.0055 compared to 0.0040; this behavior corresponds to the somewhat larger second moments of velocity fluctuations for nonbuoyant than for buoyant flows observed by Dai et al. (1995). The other moments illustrated in Fig. 3 are qualitatively similar to the results measured by Panchapakesan and Lumley (1993a) for round nonbuoyant turbulent jets.

Gradients of third moments of combined velocity/mixture fraction fluctuations determine the turbulent diffusion of scalar variance and scalar fluxes, and hence are important for estimating the scalar variance budget and developing higher-order models of turbulence. Terms of this type also appear at lower order when the governing equations are formulated using mass-weighted (Favre) averages, as advocated by Bilger (1976) for flame environments. Several of these correlations are zero due to axial symmetry, e.g., $\overline{f'u'w'} = \overline{f'v'w'} = 0$; of these, the last was measured and found to be properly equal to zero as a check of the present measurements.

Measurements of the non-zero third moments of velocity/mixture fraction fluctuations — $\overline{f'u'^2}$, $\overline{f'v'^2}$, $\overline{f'w'^2}$, $\overline{f'u'v'}$, $\overline{f'^2u'}$ and $\overline{f'^2v'}$

— are illustrated in Fig. 4, after normalization in a manner appropriate for round self-preserving buoyant turbulent plumes. Similar to other correlations, these results exhibit self-preserving behavior and least-squares fits have been found for them for later use in computing budgets. Other measurements of these properties are rare; therefore, about all that can be said is that there are qualitative similarities between present measurements and those of Panchapakesan and Lumley (1993b) for a transitional buoyant plume.

Fourth Moments. The fourth moments of velocity and velocity/mixture fraction fluctuations are needed to find appropriate expressions for the diffusion terms of triple-moment models. One approach for modeling fourth moments is to use the quasi-Gaussian approximation where fourth moments are approximated by products of second moments, as follows (Panchapakesan and Lumley, 1993a):

$$\overline{\phi_i \phi_j \phi_m \phi_n} = \overline{(\phi_i \phi_j)} \overline{(\phi_m \phi_n)} + \overline{(\phi_j \phi_m)} \overline{(\phi_i \phi_n)} + \overline{(\phi_i \phi_m)} \overline{(\phi_j \phi_n)} \quad (11)$$

where ϕ_i , etc., are generic vector or scalar fluctuating quantities. This approximation is exact if each of the fluctuating variables satisfies a Gaussian probability density function (PDF), e.g., $\overline{u^4} = 3(\overline{u^2})^2$, etc., implies a kurtosis of 3 which is correct for a Gaussian PDF of u' . In the present instance, velocity fluctuations mainly satisfy Gaussian PDF's but modifications due to intermittency must be anticipated near the edge of the flow. In addition, mixture fraction exhibits effects of intermittency because it has a finite range, $0 \leq f \leq 1$, and cannot fundamentally satisfy a Gaussian PDF, although past work suggests that a clipped-Gaussian PDF is a reasonably good approximation for its behavior (Dai et al, 1994). Thus, effects of intermittency, which penetrate clear to the axis for self-preserving round buoyant turbulent plumes (Dai et al., 1994) are an issue for present flows; therefore, efforts were made to evaluate the effectiveness of the Gaussian approximation for estimating the fourth moments of fluctuating quantities.

The fourth moments of velocity fluctuations considered during the present investigation, along with corresponding quasi-Gaussian approximations using the measurements of Dai et al. (1995) for second moments of velocity fluctuations, are illustrated in Fig. 5. Correlations considered include

$\overline{u'^4}, \overline{v'^4}, \overline{w'^4}, \overline{u'^2v'^2}, \overline{u'^2w'^2}, \overline{v'^2w'^2}$ and the sum $(\overline{u'^3v'} + \overline{u'v'^3})$ which could not be separated using the present test and LV configuration. Typical of other properties, these correlations exhibit self-preserving behavior within experimental uncertainties. Similar to the observations of Panchapakesan and Lumley (1993a) for round nonbuoyant turbulent jets, the quasi-Gaussian approximation is reasonable even though present flows exhibit significant intermittency for $r/(x-x_0) > 0.1$. Corresponding to the somewhat lower second moments of velocity fluctuations seen for buoyant turbulent plumes in comparison to nonbuoyant turbulent jets, correlations like $\overline{u'^2w'^2}$ have somewhat lower maximum values in the present buoyant turbulent plumes than in the nonbuoyant turbulent jets observed by Panchapakesan and Lumley (1993a).

The fourth moments of combined velocity/mixture fraction fluctuations considered during the present investigation, along with corresponding quasi-Gaussian approximations using both present measurements and those of Dai et al. (1994, 1995) for second moments, are illustrated in Figs. 6 and 7. Correlations considered include the first moments of f' in Fig. 6 (e.g., $\overline{f'u'^3}, \overline{f'u'v'^2}, \overline{f'u'w'^2}, \overline{f'v'^3}$ and $\overline{f'v'u'^2}$), and the higher moments of f' in Fig. 7 (e.g., $\overline{f'^2u'^2}, \overline{f'^2v'^2}, \overline{f'^2w'^2}, \overline{f'^3u'}, \overline{f'^3v'}$ and $\overline{f'^2u'v'}$). These correlations also exhibit self-preserving behavior and are in reasonably good agreement with the quasi-Gaussian approximation, within experimental uncertainties, in spite of anticipated effects of intermittency for $r/(x-x_0) > 0.1$. Finally, several fourth order moments that should be zero due to symmetry, e.g., $\overline{f'w'^3}, \overline{f'u'^2w'}, \overline{f'^2u'w'}$ and $\overline{f'^3w'}$ were measured, and were all properly found to be

equal to zero within experimental uncertainties as a check of the measurements.

Budgets. Budgets of turbulence kinetic energy and scalar variance were considered in order to provide estimates of the rates of dissipation which were not measured directly during the experiments, and to highlight the mechanisms of turbulent mixing in buoyant turbulent flows. Properties needed to compute budgets were found from Dai et al. (1994, 1995) and the present study. The procedure involved using the general expressions of Eqs. (2)-(6) for \bar{u} and \bar{f} , along with the local least-squares fits illustrated on the plots of other properties.

The governing equations for the turbulence kinetic energy, $k = (\bar{u}'^2 + \bar{v}'^2 + \bar{w}'^2)/2$, and the scalar variance, $g = \bar{f}'^2$, were found at the high Reynolds number limits appropriate for present experimental conditions where direct effects of molecular diffusion can be ignored. In order to simplify the following discussion, it was assumed that $\bar{v}'^2 = \bar{w}'^2$ which is a good approximation for present flows based on the measurements of Dai et al. (1995). Under these approximations, the governing equation for turbulence kinetic energy can be written as follows (Panchapakesan and Lumley, 1993b):

$$\bar{u}\partial k / \partial x + \bar{v}\partial k / \partial r = D + T + P + G - \epsilon \quad (12)$$

where

$$D = -\partial / \partial x (\bar{u}'k) - \partial / \partial r (r \bar{v}'k) / r \quad (13)$$

$$T = -\partial / \partial x (\bar{p}'u') - \partial / \partial r (r \bar{p}'v') / r \quad (14)$$

$$P = -(\bar{u}'^2 - \bar{v}'^2)\partial \bar{u} / \partial x - \bar{u}'v'(\partial \bar{u} / \partial r + \partial \bar{u} / \partial x) \quad (15)$$

$$G = (1 - \rho_\infty / \rho_0) a \bar{f}'u' \quad (16)$$

The terms on the left hand side (LHS) of Eq. (12) represent advection while the terms on the right hand side (RHS) represent turbulent diffusion (diffusion), pressure diffusion,

mechanical production (production), buoyancy production and dissipation, respectively.

Present determinations of the terms in the equation of conservation of turbulence kinetic energy for the self-preserving region are plotted in Fig. 8. Each term in the plots has been made dimensionless by multiplying it by $(x-x_0)/\bar{u}_c^3$, which is consistent with self-preserving scaling. In this case, the radial production, the total production (production), the buoyancy production, the advection, the total diffusion (diffusion) and the radial diffusion terms have been found directly from the measurements. In contrast, the sum of dissipation plus pressure diffusion (which is labeled dissipation in the figure) has been found from the budget as a balance. In the following, the pressure diffusion effect will be ignored and the sum will be treated as dissipation alone similar to other treatments of turbulent flows having nearly constant density (Panchapakesan and Lumley (1993a,b; Shih et al., 1987). The radial and total production terms, and the radial and total diffusion terms, are nearly the same as expected for a boundary layer flow. Near the axis, advection, radial diffusion and buoyancy production are all roughly the same, and their sum is balanced by dissipation. The profiles of production, diffusion and dissipation are qualitatively similar to the results reported by Panchapakesan and Lumley (1993a) for nonbuoyant turbulent jets, however, advection near the axis is much smaller for plumes than for jets (by a factor of 2-3) which is compensated by contributions from buoyancy production and diffusion for the plumes.

Under the same approximations as the k equation, the governing equations for the scalar variance can be written as follows (Panchapakesan and Lumley, 1993b):

$$\bar{u}\partial g/\partial x + \bar{v}\partial g/\partial r = D_g + P_g - 2\varepsilon_g \quad (17)$$

where

$$D_g = -\partial/\partial x(\bar{u}'g) - \partial/\partial r(r\bar{v}'g)/r \quad (18)$$

$$P_g = -2\bar{f}'u'\partial\bar{f}/\partial x - 2\bar{f}'v'\partial\bar{f}/\partial r \quad (19)$$

The term on the LHS of Eq. (17) is the advection while the terms on the RHS are the turbulent

diffusion (diffusion), mechanical production (production) and dissipation, respectively.

Present determinations of the terms in the equation for scalar variance for the self-preserving region are plotted in Fig. 9. Each term in the plots has been made dimensionless by multiplying it by $(x-x_0)/(\bar{f}'^2\bar{u}_c)$, which is consistent with self-preserving scaling. In this case, the advection, the total production (production), the radial production, the total diffusion (diffusion), and the radial diffusion have been found directly from the measurements. In contrast, the dissipation has been found from the budget as a balance. Radial and total diffusion are nearly the same which is typical of a boundary-layer flow. In contrast, streamwise and radial production are only comparable near the edge of the flow, while streamwise production dominates near the axis, as discussed earlier, due to the large streamwise gradient of \bar{f} and large values of $\bar{f}'u'$ in this region. It is likely that this large level of streamwise production near the axis is responsible for the large values of scalar variance in this region, see Dai et al. (1994). Near the axis, advection (with smaller contributions from production and diffusion) is balanced by dissipation. Near the edge of the flow, however, advection becomes small and radial production balances diffusion. These trends are similar to the observations of Panchapakesan and Lumley (1993b) for a transitional buoyant turbulent jet, except that the present flows have larger contributions to advection, balanced by increased dissipation, near the axis.

Present estimates of ε and ε_g from Figs. 8 and 9 are helpful for studying approximations used in turbulence models. Two parameters of interest that will be considered are the ratio of the characteristic velocity to mixture-fraction time scales, C_{g2} , and the constant in the gradient diffusion approximation for the Reynolds stress, C_{μ} . These two properties can be evaluated, as follows:

$$C_{g2} = \varepsilon_g k/(\varepsilon g) \quad (20)$$

and

$$C_{\mu} = -\varepsilon \overline{u'v'} / (k^2 \partial \bar{u} / \partial r) \quad (21)$$

Continuing the approximation that the pressure diffusion terms can be ignored when evaluating ε , the present measurements and those of Dai et al.(1994, 1995) provide all the properties on the RHS of Eqs. (20) and (21) which allows C_{g2} and C_{μ} to be evaluated. The resulting measured values of C_{g2} and C_{μ} are summarized as a function of $r/(x-x_0)$ in Table 1. Analogous to the turbulent Prandtl/Schmidt number, the values of C_{g2} and C_{μ} vary considerably as $r/(x-x_0)$ varies, rather than remaining constant in accord with the approximations of simple turbulence models. Near the axis, however, C_{g2} is in the range 1.96-2.56, which is comparable to the value of this constant used in simple turbulence models where C_{g2} is in the range 1.87-1.92, see Lockwood and Naguib (1975). Similarly, values of C_{μ} near the axis are 0.10-0.11 which also is comparable to the widely used value, $C_{\mu} = 0.09$, see Lockwood and Naguib (1975). The reasons for the variation of C_{g2} and C_{μ} with increasing $r/(x-x_0)$ are not known but probably are associated with the corresponding variation of intermittency. In any event, these findings concerning C_{g2} and C_{μ} also support the need for higher-order closures to reliably treat effects of flow development within buoyant turbulent flows. The various measurements of higher-order moments reported here should be helpful for efforts along these lines.

CONCLUSIONS

Velocity/mixture fraction statistics and other higher-order turbulence quantities were measured within self-preserving of round buoyant turbulent plumes in still and unstratified air, in order to supplement earlier measurements of mixture fraction and velocity statistics for these flows due to Dai et al.(1994, 1995). Test conditions involved buoyant jet sources of carbon dioxide and sulfur hexafluoride to give ρ_0 / ρ_{∞} of 1.51 and 5.06 and source Froude numbers of 7.80 and 3.75, respectively, with $(x-x_0)/d$ in the range 87-151 and $(x-x_0)/\ell_M$ in the range 12-43. The major conclusions of the study are as follows:

1. All moments observed during the present investigation exhibited self-preserving

behavior within experimental uncertainties over the test range, similar to the earlier observations of Dai et al.(1994, 1995). This included the following variables: $\overline{f'u'}$, $\overline{f'v'}$, σ_T , $\overline{u'^3}$, $\overline{u'v'^2}$, $\overline{u'w'^2}$, $\overline{v'u'^2}$, $\overline{v'v'^2}$, $\overline{v'w'^2}$, $\overline{f'u'^2}$, $\overline{f'v'^2}$, $\overline{f'w'^2}$, $\overline{f'^2u'}$, $\overline{f'^2v'}$, $\overline{f'u'v'}$, $\overline{u'^4}$, $\overline{v'^4}$, $\overline{w'^4}$, $\overline{u'^2v'^2}$, $\overline{u'^2w'^2}$, $\overline{v'^2w'^2}$, $\overline{(u'v'^3 + u'^3v')}$, $\overline{f'u'^3}$, $\overline{f'u'v'^2}$, $\overline{f'u'w'^2}$, $\overline{f'v'^3}$, $\overline{f'v'u'^2}$, $\overline{f'^2u'^2}$, $\overline{f'^2v'^2}$, $\overline{f'^2w'^2}$, $\overline{f'^3u'}$, $\overline{f'^3v'}$ and $\overline{f'^2u'v'}$.

2. Streamwise turbulent fluxes of mass and momentum exhibited countergradient diffusion for $r/(x-x_0) \geq 0.082$ and 0.042 , respectively, although the much more significant radial fluxes of these properties satisfied gradient diffusion in the normal manner for the present boundary layer flows. Nevertheless, even though the countergradient diffusion deficiency is not very important for self-preserving round turbulent plumes, it raises concerns about the use of simple gradient diffusion hypotheses for more complex buoyant turbulent flows of interest in practice.
3. The turbulent Prandtl/Schmidt number, the ratio of characteristic velocity to mixture fraction time scales and the coefficient of the radial gradient diffusion approximation for Reynolds stress, all exhibited significant variations across the flow rather than remaining constant as prescribed by simple turbulence models. These variations tend to parallel the variation of intermittency so that the presence of nonturbulent fluid may be responsible for the behavior. These variations of flow properties also point to the need for higher-order model closures in order to reliably treat effects of flow development within buoyant turbulent flows.
4. Fourth moments of velocity and velocity/mixture fraction fluctuations generally satisfied the quasi-Gaussian approximation across the flow width. This behavior also has been observed by Panchapakesan and Lumley (1993a,b) for nonbuoyant and buoyant jets but it still was

surprising in view of potential effects of intermittency and the departure of the PDF of mixture fraction from Gaussian behavior near the edge of the flow.

5. Streamwise turbulent mass fluxes are quite large near the axis in buoyant turbulent plumes, where the corresponding correlation coefficients are roughly 0.7. This behavior, combined with the rapid decay of mean mixture fraction in the streamwise direction, is a strong source of production of scalar fluctuations, which probably is responsible for the large values of mixture fraction fluctuation intensities, roughly 0.45, observed near the axis of self-preserving round buoyant turbulent plumes.

ACKNOWLEDGMENTS

This research was supported by the United States Department of Commerce, National Institute of Standards and Technology, Grant Nos. 60NANB1D1175 and 60NANB4D1234, with H. R. Baum and K. C. Smyth of the Building and Fire Research Laboratories serving as Scientific Officers.

REFERENCES

- Abraham, G., 1960, "Jet Diffusion in Liquid of Greater Density," ASCE J. Hyd. Div., Vol. 86, pp. 1-13.
- Bilger, R.W., 1976, "Turbulent Jet Diffusion Flames," Prog. Energy Combust. Sci., Vol. 1, pp. 87-109.
- Chen, C.J., and Rodi, W., 1980, *Vertical Turbulent Buoyant Jets: A Review of Experimental Data.*, Pergamon Press, Oxford, p. 16.
- Dai, Z., Tseng, L.-K., and Faeth, G.M., 1994, "Structure of Round, Fully-Developed, Buoyant Turbulent Plumes," J. Heat Trans., Vol. 116, pp. 409-417.
- Dai, Z., Tseng, L.-K., and Faeth, G.M., 1995, "Velocity Statistics of Round, Fully-Developed Buoyant Turbulent Plumes," J. Heat Transfer, in press.
- George, W.K., Jr., Alpert, R.L., and Tamanini, F., 1977, "Turbulence Measurements in an Axisymmetric Buoyant Plume," Int. J. Heat Mass Trans., Vol. 20, pp. 1145-1154.
- Hinze, J. O., 1975, *Turbulence*, 2nd ed., McGraw-Hill, New York, pp. 175-319.
- Kotsovinos, N.E., 1985, "Temperature Measurements in a Turbulent Round Plume," Int. J. Heat Mass Trans., Vol. 28, pp. 771-777.
- Lai, M.-C., and Faeth, G.M., 1987, "A Combined Laser-Doppler Anemometer/Laser-Induced Fluorescence System for Turbulent Transport Measurements," J. Heat Trans., Vol. 109, pp. 254-256.
- List, E.J., 1982, "Turbulent Jets and Plumes," Ann. Rev. Fluid Mech., Vol. 14, pp. 189-212.
- Lockwood, F.C., and Naguib, A.S., 1975, "The Prediction of Fluctuations in the Properties of Free, Round-Jet Turbulent Diffusion Flames," Combust. Flame, Vol. 24, pp. 109-124.
- Lumley, J.L., 1978, "Computational Modeling of Turbulent Flows," Adv. Appl. Mech., Vol. 18, pp. 123-176.
- Malin, M.R., and Younis, B.A., 1990, "Calculation of Turbulent Buoyant Plumes with a Reynolds Stress and Heat Flux Transport Closure," Int. J. Heat Mass Trans., Vol. 33, pp. 2247-2264.
- Mizushima, T., Ogino, F., Veda, H., and Komori, S., 1979, "Application of Laser-Doppler Velocimetry to Turbulence Measurements in Non-Isothermal Flow," Proc. Roy. Soc. London, Vol. A366, pp. 63-79.
- Morton, B.R., 1959, "Forced Plumes," J. Fluid Mech., Vol. 5, pp. 151-163.
- Morton, B.R., Taylor, G.I., and Turner, J.S., 1956, "Turbulent Gravitational Convection from Maintained and Instantaneous Sources," Proc. Roy. Soc. London, Vol. A234, pp. 1-23.

- Nakagome, H., and Hirata, M., 1977, "The Structure of Turbulent Diffusion in an Axi-Symmetrical Thermal Plume," *Heat Transfer and Turbulent Buoyant Convection* (D.B. Spalding and N. Afgan, eds.), McGraw-Hill, New York, pp. 367-372.
- Ogino, F., Takeuchi, H., Kudo, I., and Mizushima, T., 1980, "Heated Jet Discharged Vertically in Ambients of Uniform and Linear Temperature Profiles," *Int. J. Heat Mass Trans.*, Vol. 23, pp. 1581-1588.
- Panchapakesan, N.R., and Lumley, J.L., 1993a, "Turbulence Measurements in Axisymmetric Jets of Air and Helium. Part. 1. Air Jet," *J. Fluid Mech.*, Vol. 246, pp. 197-223.
- Panchapakesan, N.R., and Lumley, J.L., 1993b, "Turbulence Measurements in Axisymmetric Jets of Air and Helium. Part 2. Helium Jet," *J. Fluid Mech.*, Vol. 246, pp. 225-247.
- Papanicolaou, P.N., and List, E.J., 1987, "Statistical and Spectral Properties of Tracer Concentration in Round Buoyant Jets," *Int. J. Heat Mass Trans.*, Vol. 30, pp. 2059-2071.
- Papanicolaou, P.N., and List, E.J., 1988, "Investigation of Round Vertical Turbulent Buoyant Jets," *J. Fluid Mech.*, Vol. 195, pp. 341-391.
- Papantoniou, D., and List, E.J., 1989, "Large Scale Structure in the Far Field of Buoyant Jets," *J. Fluid Mech.*, Vol. 209, pp. 151-190.
- Peterson, J., and Bayazitoglu, Y., 1992, "Measurements of Velocity and Turbulence in Vertical Axisymmetric Isothermal and Buoyant Plumes," *J. Heat Trans.*, Vol. 114, pp. 135-142.
- Rouse, H., Yih, C.S., and Humphreys, H.W., 1952, "Gravitational Convection from a Boundary Source," *Tellus*, Vol. 4, pp. 201-210.
- Seban, R.A., and Behnia, M.M., 1976, "Turbulent Buoyant Jets in Unstratified Surroundings," *Int. J. Heat Mass Trans.*, Vol. 19, pp. 1197-1204.
- Shabbir, A., and George, W.K., 1992, "Experiments on a Round Turbulent Buoyant Plume," NASA Technical Memorandum 105955.
- Shabbir, A., and Taulbee, D.B., 1990, "Evaluation of Turbulence Models for Predicting Buoyant Flows," *J. Heat Trans.*, Vol. 112, pp. 945-951.
- Shih, T.-H., Lumley, J.L., and Janicka, J., 1987, "Second-Order Modeling of a Variable-Density Mixing Layer," *J. Fluid Mech.*, Vol. 180, pp. 93-116.
- Taulbee, D.B., 1992, "An Improved Algebraic Reynolds Stress Model and Corresponding Nonlinear Stress Model," *Phys. Fluids A*, Vol. 4, pp. 2555-2561.
- Tennekes, H., and Lumley, J.L., 1972, *A First Course in Turbulence*, MIT Press, Cambridge, Massachusetts.
- Zimin, V.D., and Frik, P.G., 1977, "Averaged Temperature Fields in Asymmetrical Turbulent Streams over Localized Heat Sources," *Izv. Akad. Nauk. SSSR. Mekhanika Zhidkosti Gaza*, Vol. 2, pp. 199-203.

TABLE 1. SUMMARY TURBULENCE MODEL PARAMETERS

$r/(x-x_0)$	0.00	0.05	0.10	0.15	0.20
C_{g2}^a	2.56	1.96	3.70	4.55	4.17
C_{μ}^b	0.10	0.11	0.043	0.031	0.040

^aRatio of characteristic velocity to mixture-fraction time scales,

$$C_{g2} = \epsilon_g k / (\epsilon g).$$

^bTurbulence modeling constant, $C_{\mu} = -\epsilon \overline{u'v'} / (k^2 \partial \bar{u} / \partial r)$.

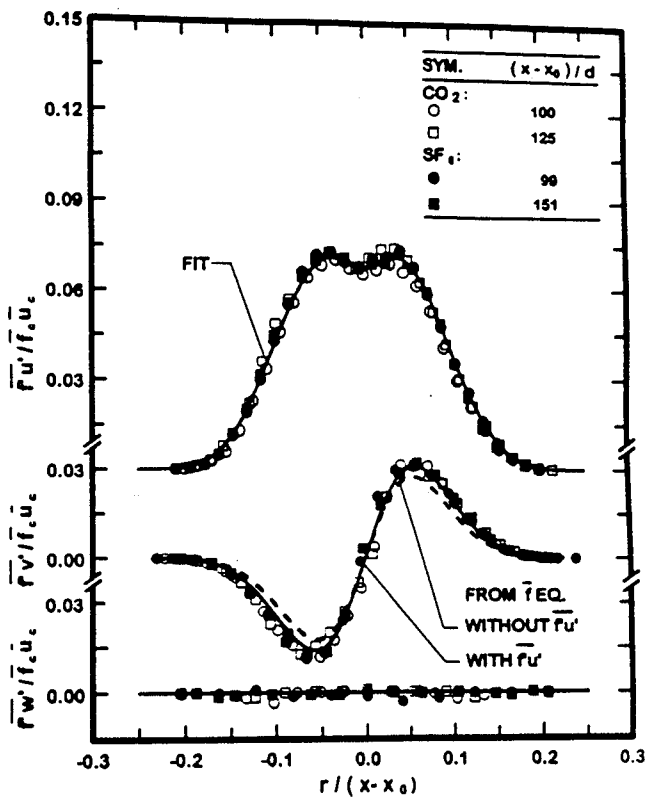


Fig. 1 Radial distributions of turbulent mass fluxes within self-preserving buoyant turbulent plumes.

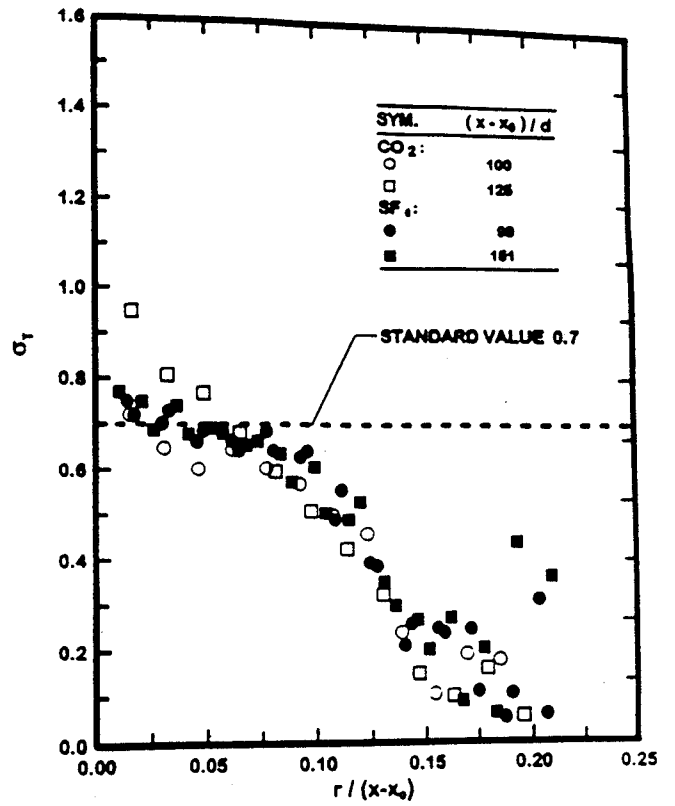


Fig. 2 Radial distribution of turbulent Prandtl/Schmidt numbers within self-preserving buoyant turbulent plumes.

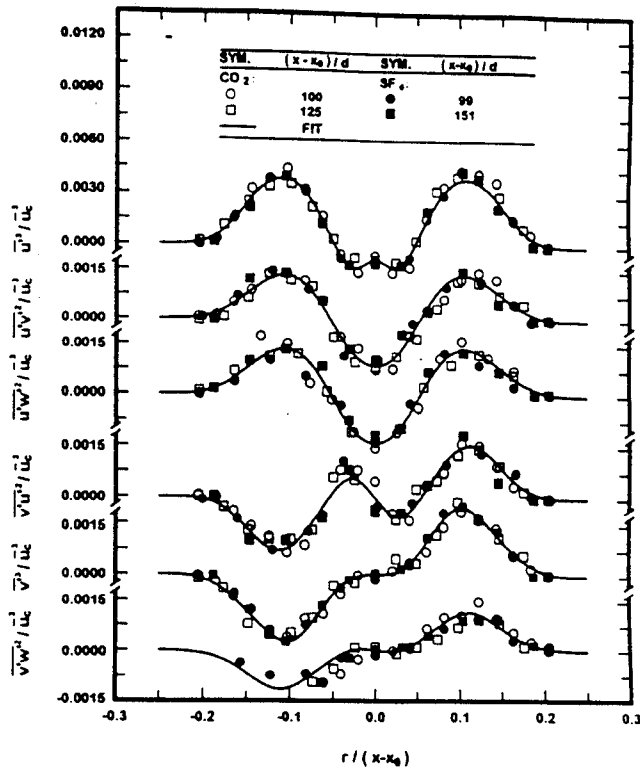


Fig. 3 Radial distribution of triple moments of velocity fluctuations within self-preserving buoyant turbulent plumes.

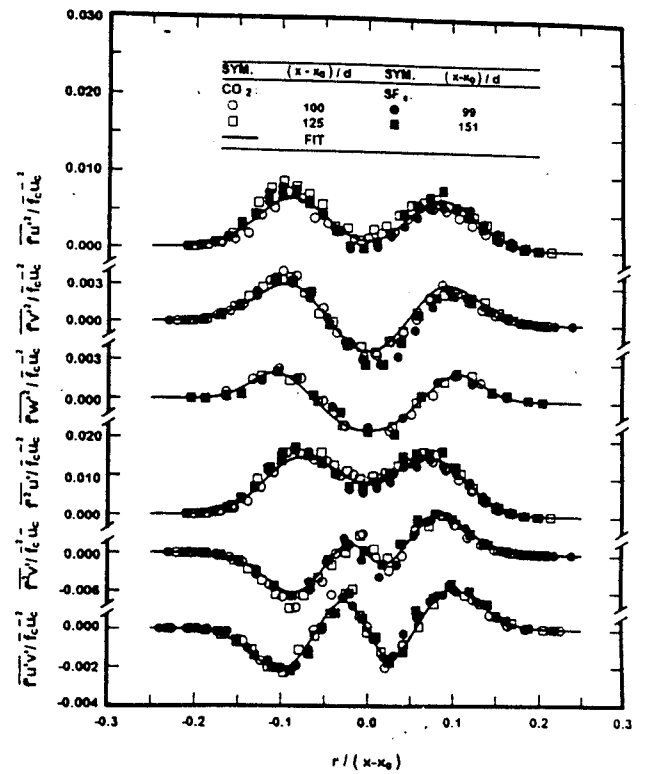


Fig. 4 Radial distribution of triple moments of velocity-mixture fraction fluctuations within self-preserving buoyant turbulent plumes.

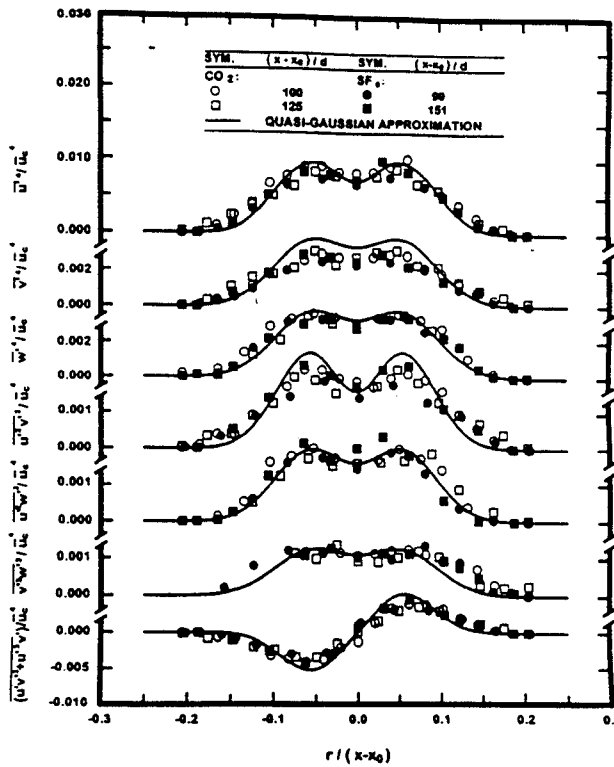


Fig. 5 Radial distribution of fourth moments of velocity fluctuations within self-preserving buoyant turbulent plumes.

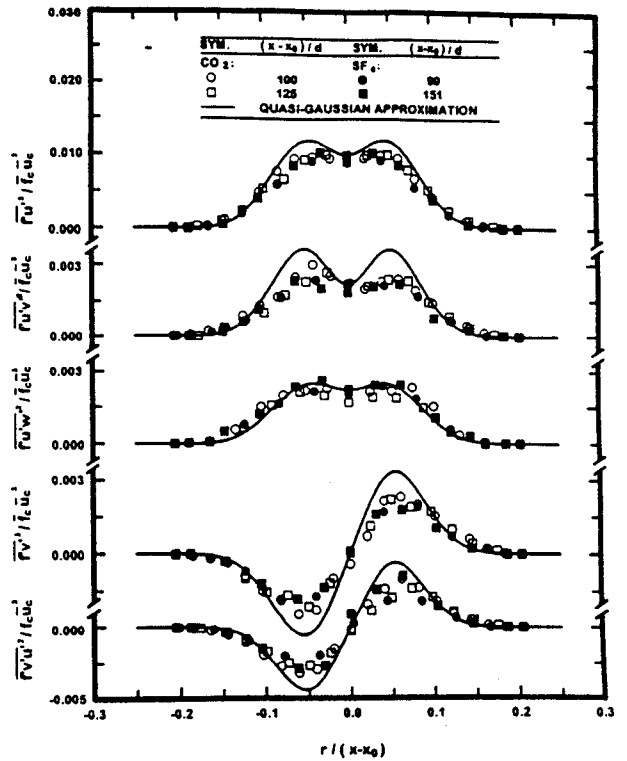


Fig. 6 Radial distribution of fourth moments of velocity-mixture fraction fluctuations involving first moments of mixture fraction fluctuations within self-preserving buoyant turbulent plumes.

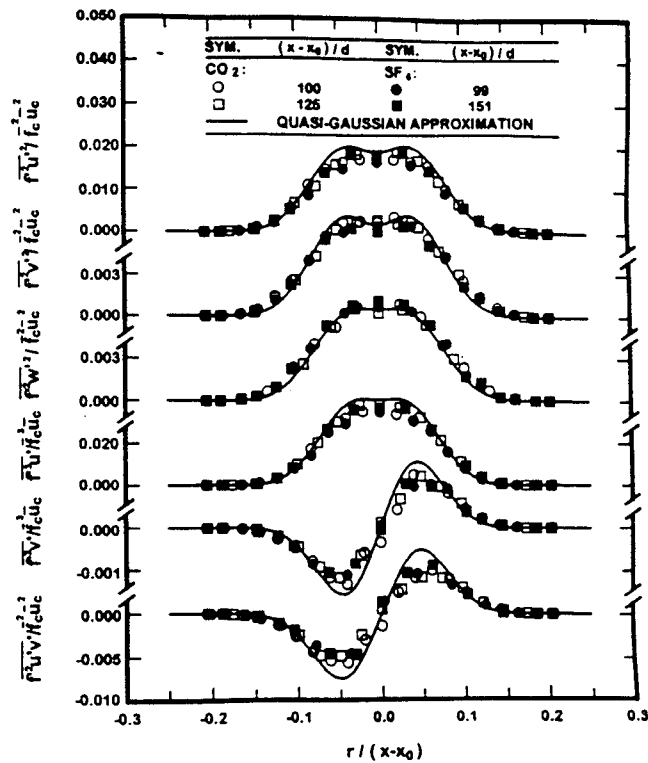


Fig. 7 Radial distribution of fourth moments of velocity and higher-order moments of mixture-fraction fluctuations within self-preserving buoyant turbulent plumes.

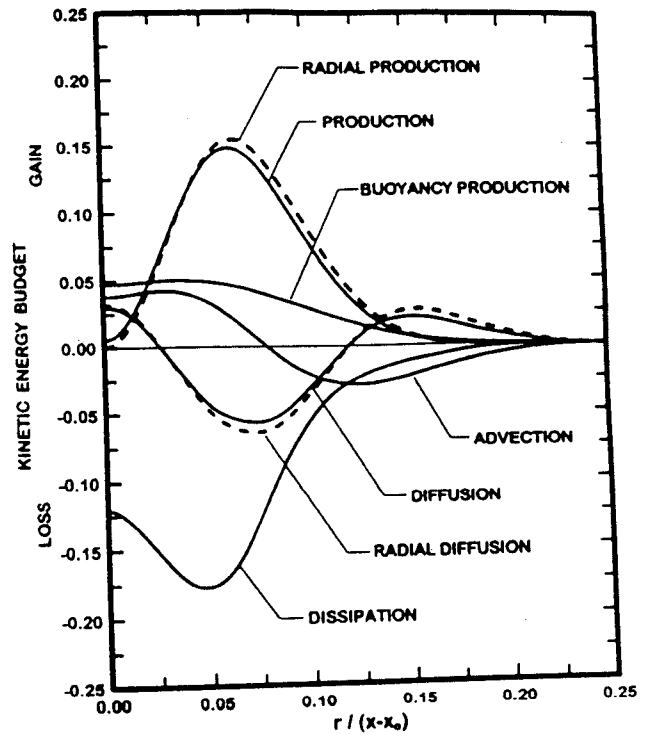


Fig. 8 Turbulence kinetic energy budget within self-preserving buoyant turbulent plumes.

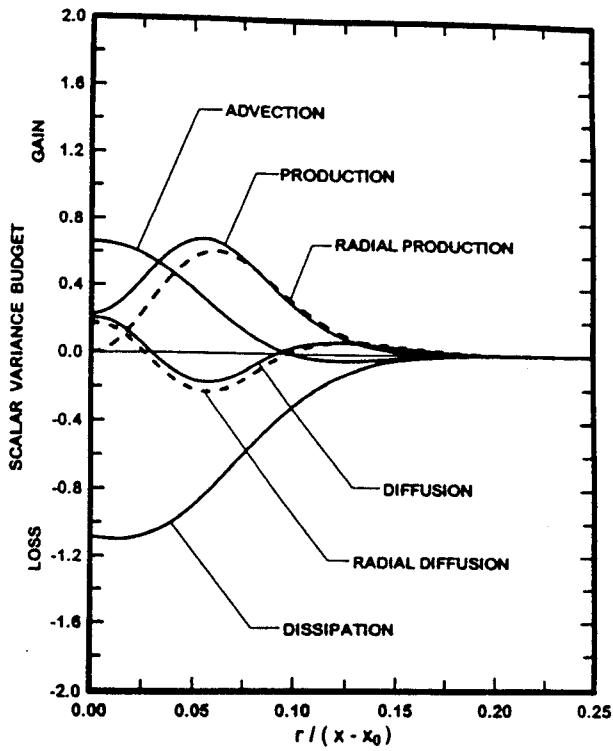


Fig. 9 Mixture fraction fluctuation budget within self-preserving buoyant turbulent plumes.